SYSTEMS TECHNOLOGY, INC

13766 S. HAWTHORNE BOULEVARD • HAWTHORNE, CALIFORNIA 90250-7083 • PHONE (310) 679-2281
email: sti@systemstech.com FAX (310) 644-3887

Working Paper 1439-2

Classical Control Design Feasibility Study with BFF Models

Started: November 17, 2014
Latest Revision: November 18, 2014

Dongchan Lee
Principal Specialist
310.679.2281x130

Brian P. Danowsky
Principal Research Engineer
310.679.2281x128

Prepared for

NASA NRA Grant:
Performance Adaptive Aeroelastic Wing
Contract No. NNX14AL36A

This page intentionally left blank

1.0 INTRODUCTION

This working paper documents an initial control feasibility study to determine if classical control techniques could be utilized to favorably augment the stability of the BFF vehicle. This study focused on the lower speed models which have stable, or slightly unstable aeroelastic dynamics. Future studies will explore the higher speed models with highly unstable aeroelastic modes. The final control solution will incorporate stability augmentation with aeroelastic suppression, including flutter suppression to stabilize the vehicle beyond the flutter boundary. The principal goal is a defined strategy, process and supporting software tools to develop a full envelope controller for flexible aeroelastic vehicles with significant rigid body and flexible coupling. Focus will be on blended wing-body vehicle designs like the BFF and X-56A. The purpose of this study is a background feasibility investigation.

2.0 CONTROL DESIGN STUDIES

2.1 *Controller Design for the Model at 40 kts.*

Open Loop System

A block diagram of the open loop system is shown in Figure 1.

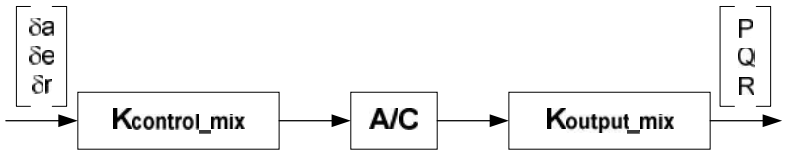

Figure 1: Open Loop System

There are 8 trailing edge surfaces that are combined into effective aileron, elevator, and rudder. The thrust inputs were not used. The roll, pitch, and yaw rate outputs were selected.

Control Allocation

The bare airframe system survey starts with control allocation to reduce 8 control surfaces to equivalent aileron, elevator and rudder inputs through the following relationship to compute ganging matrix K,

$$K = W_u^{-1}(CB)^T\left[(CB)W_u^{-1}(CB)^T\right]^{-1} \tag{1}$$

where W_u is a weighting matrix (usually diagonal) on the bare airframe inputs, C is the state space output matrix that selects the controlled variables (p, q, r) and B is the input matrix. This definition is only valid if CB is not zero (see Ref. [1]). To avoid CB being zero the actuator states are removed from the full model using the residualization technique. Figure 2 shows the control ganging K (using $W_u = I$) for the system at 40 kts flight (columns of K are plotted vs. bare airframe input). In Figure 2, it is shown that the control effectiveness of equivalent rudder is negligible compared to equivalent aileron and elevator. This is intuitive since there are no vertical control surfaces on this vehicle, like a traditional rudder.

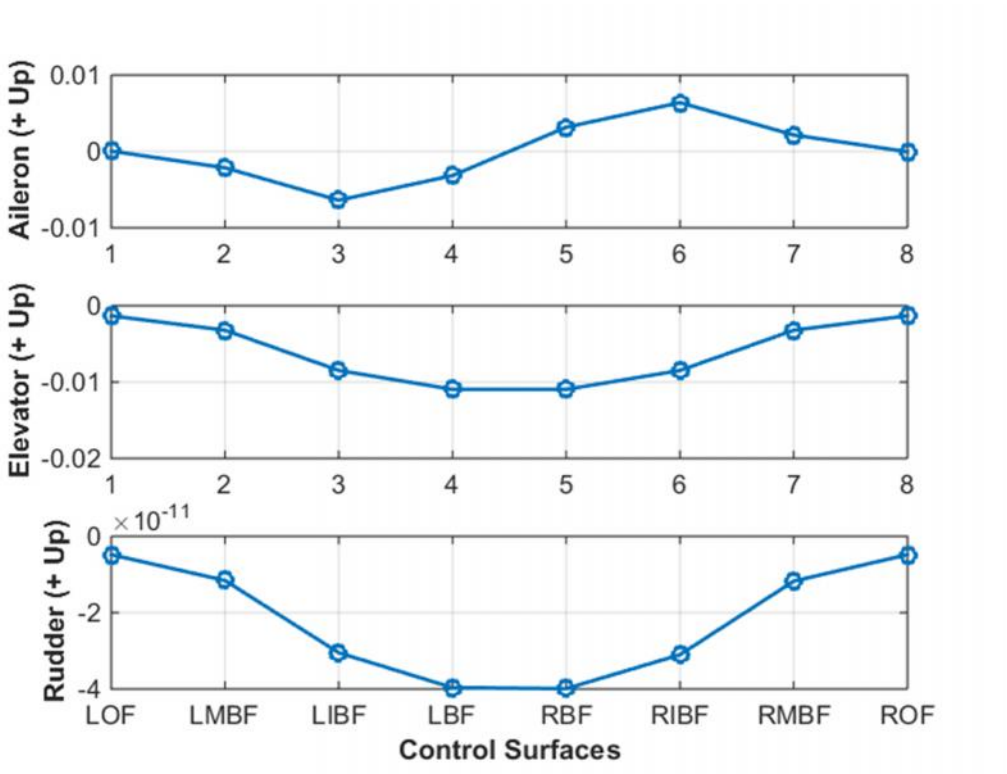

Figure 2: Control Allocation Example (40 kts Case).

Controller Design

Figure 3 to Figure 5 are Bode plots from each equivalent control surface to the roll, pitch, and yaw rates. It is shown in Figure 5 that the rudder effectiveness on each angular rate is negligible compared to other two equivalent control surfaces. From the frequency response plots, the identified two most important rigid body modes are,

- **stable short-period mode:** $\mu_n = 22.1$ rad/sec, $\zeta = 0.512$
- **stable dutch-roll mode:** $\mu_n = 3.12$ rad/sec, $\zeta = 0.101$

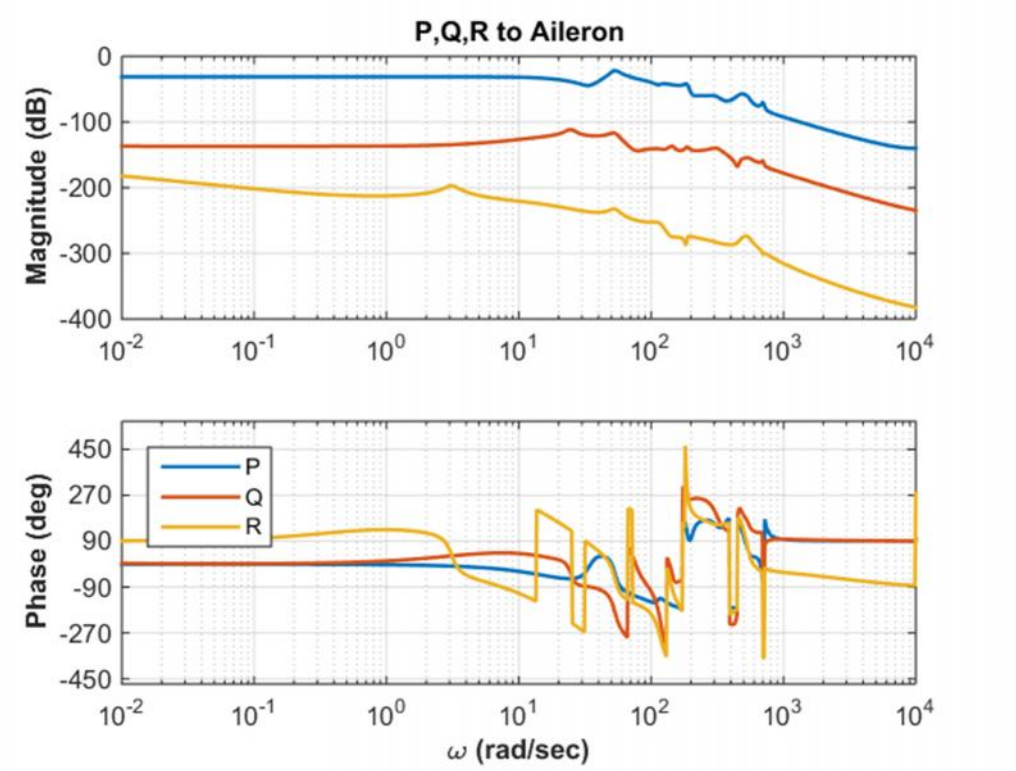

Figure 3: Bare Airframe Frequency Responses from Aileron (40 kts Case).

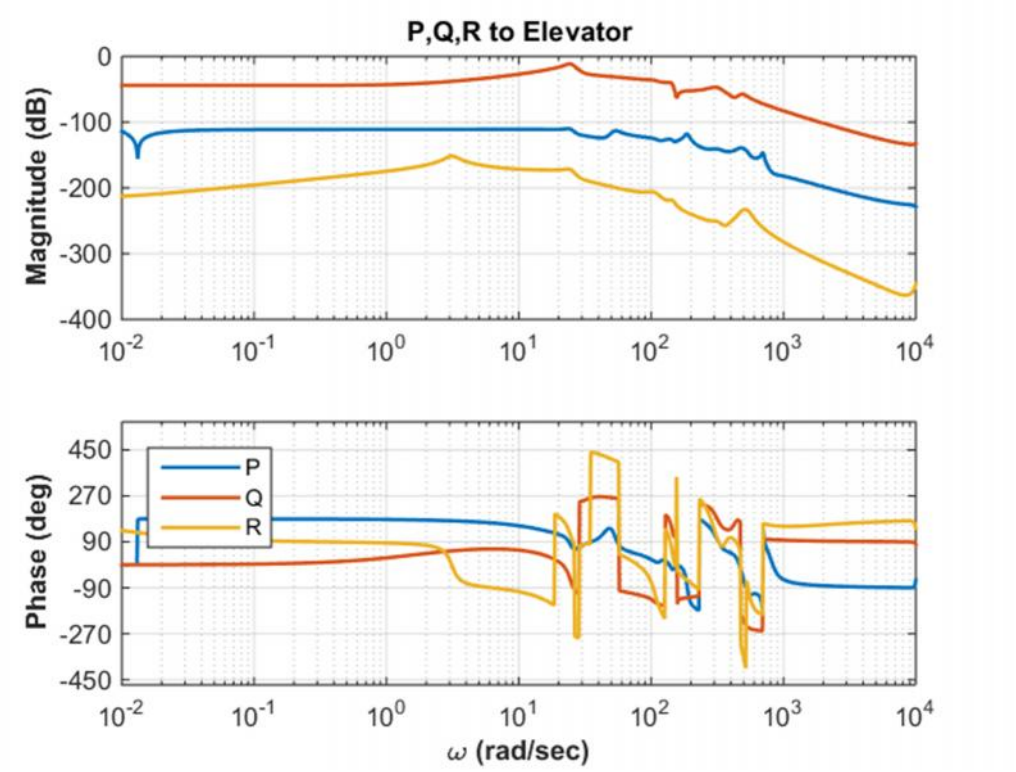

Figure 4: Bare Airframe Frequency Responses from Elevator (40 kts Case).

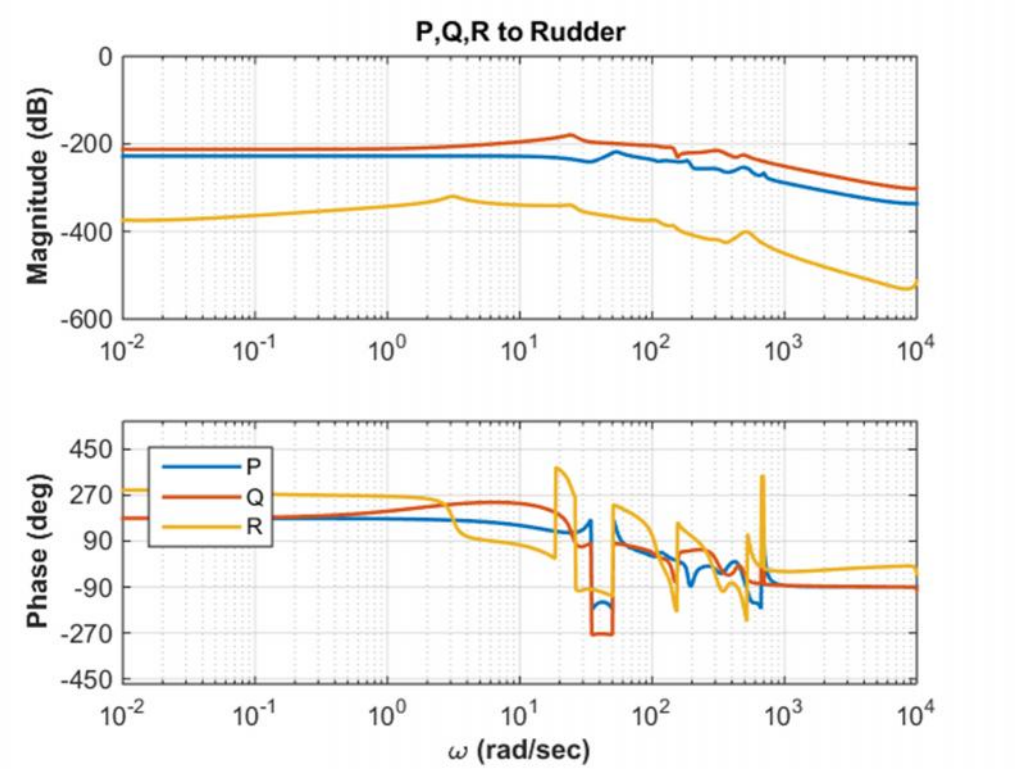

Figure 5: Bare Airframe Frequency Responses from Rudder (40 kts Case).

Step response of roll, pitch, and yaw rates are presented in Figure 6 to Figure 8. The open-loop system is stable and each angular rate reaches steady state. However, they show poor command tacking performance. A successive loop-closure technique is applied to improve command tracking performance as well as to provide primary Stability Augmentation Systems on each axis. The primary control system structure is based on Proportional-Integral controller with second order poles at the origin. Only the effective aileron and elevator were used for feedback. The effective rudder, which has negligible effect as displayed, was not used to augment stability. The tunable parameter is cross-over frequency.[2] For these controllers, the cross-over frequency was set to 10 rad/s for the roll axis and 5 rad/s for the pitch axis.

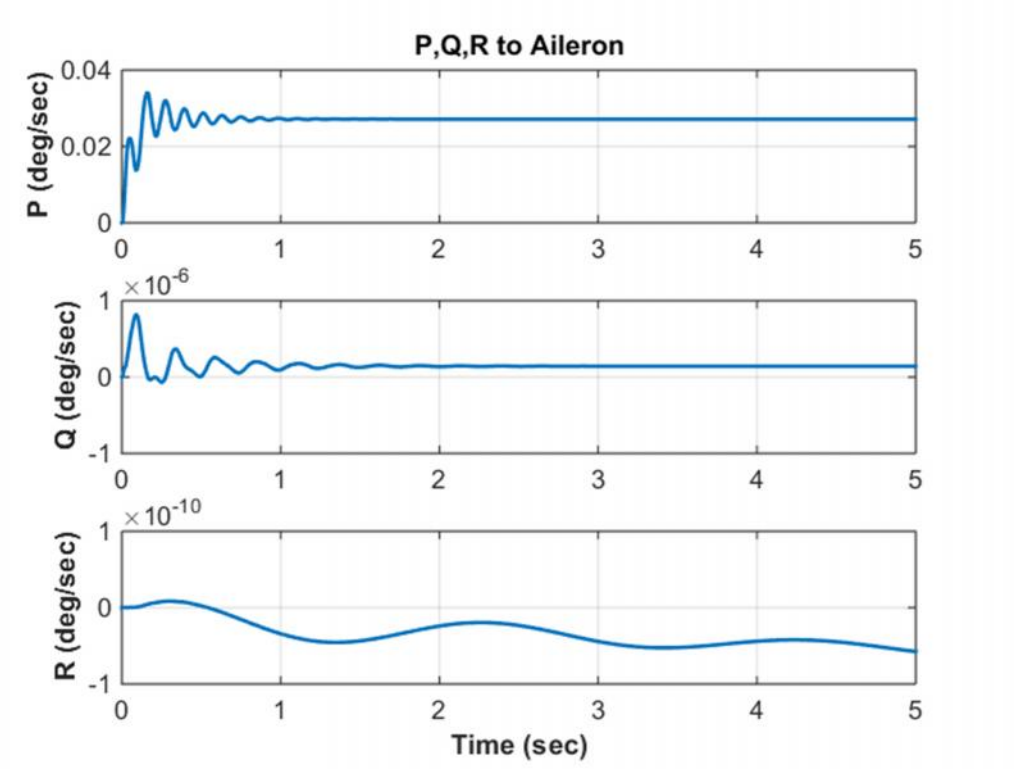

Figure 6: Bare Airframe Step Responses from Aileron (40 kts Case).

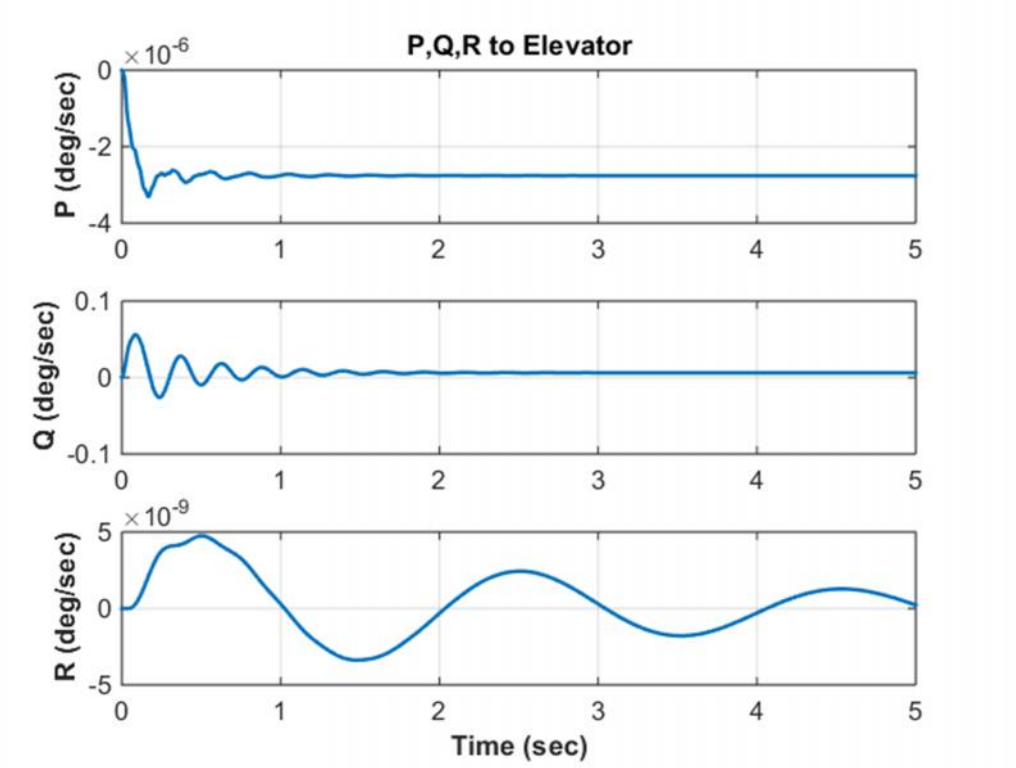

Figure 7: Bare Airframe Step Responses from Elevator (40 kts Case).

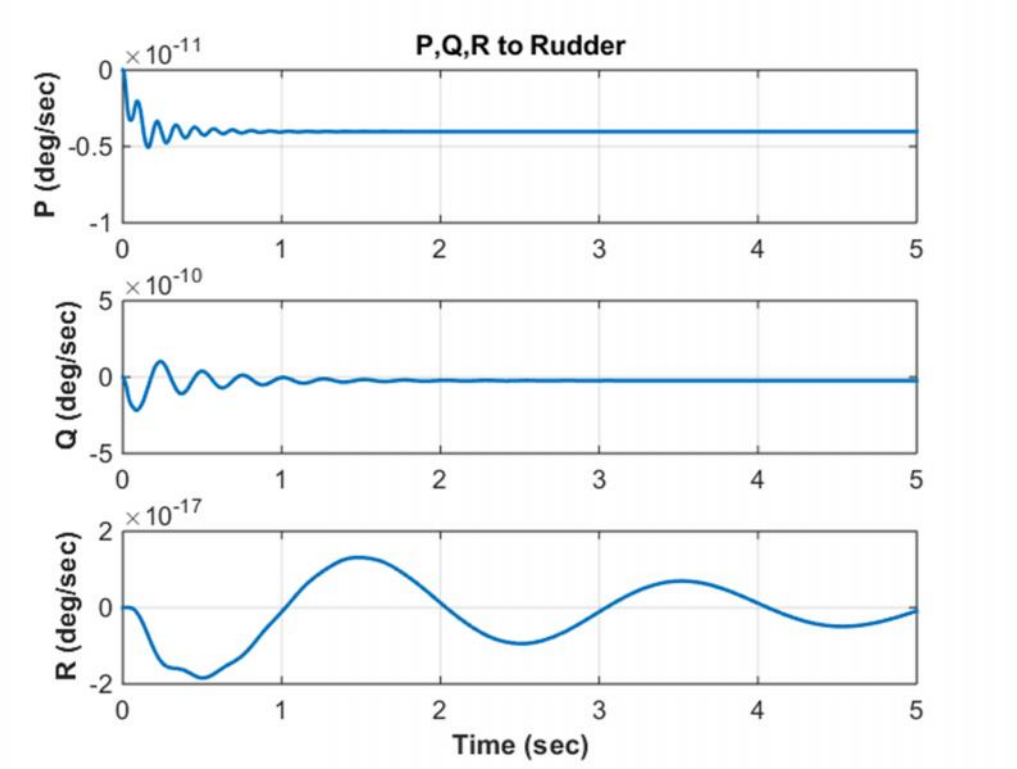

Figure 8: Bare Airframe Step Responses from Rudder (40 kts Case).

Figure 9 to Figure 11 shows the step responses of roll, pitch, and yaw rates to aileron, elevator, and rudder inputs. It is shown that the SAS provided an improved tracking performance along with significantly reduced oscillation in each rate response. The bode plots of the three angular rates (shown in Figure 12 to Figure 14) indicate that the dominant short period mode and the anti-symmetric wing 1st Bending modes at 54 rad/sec were successfully suppressed.

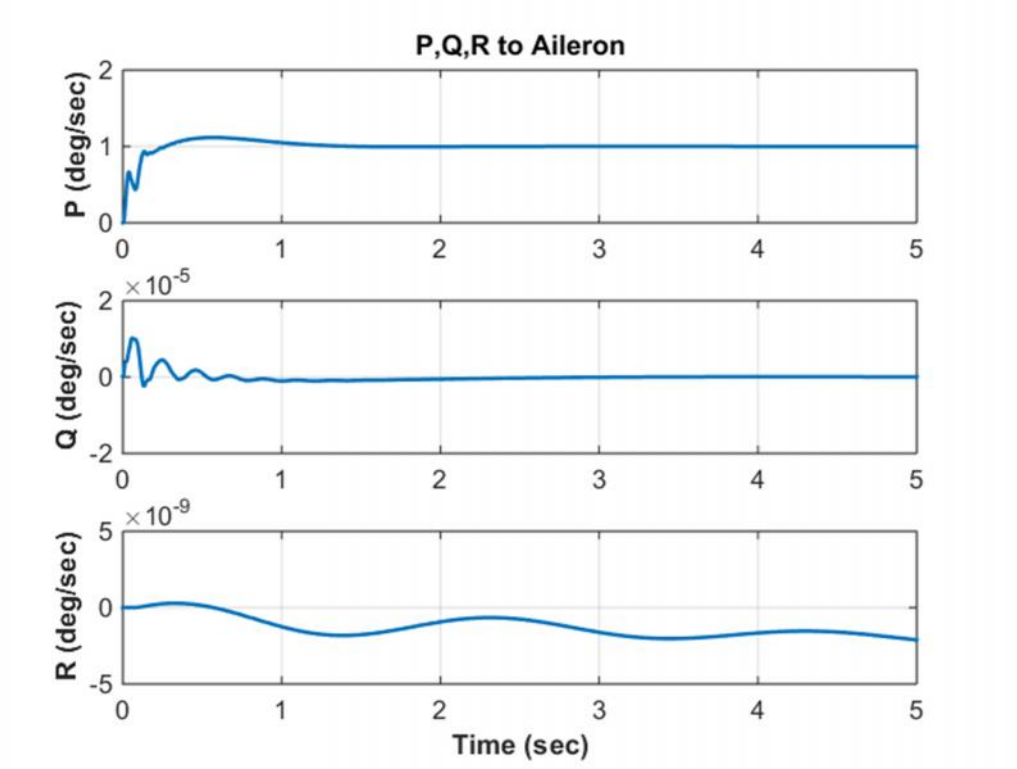

Figure 9: Closed-Loop Step Responses from Aileron (40 kts Case).

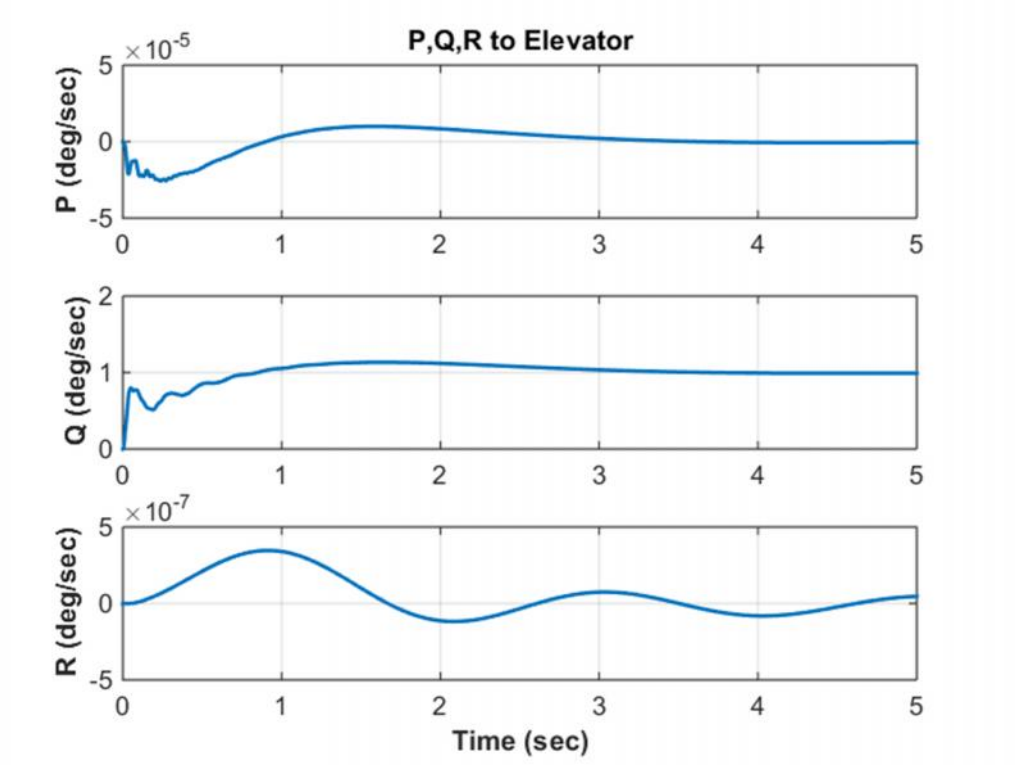

Figure 10: Closed-Loop Step Responses from Elevator (40 kts Case).

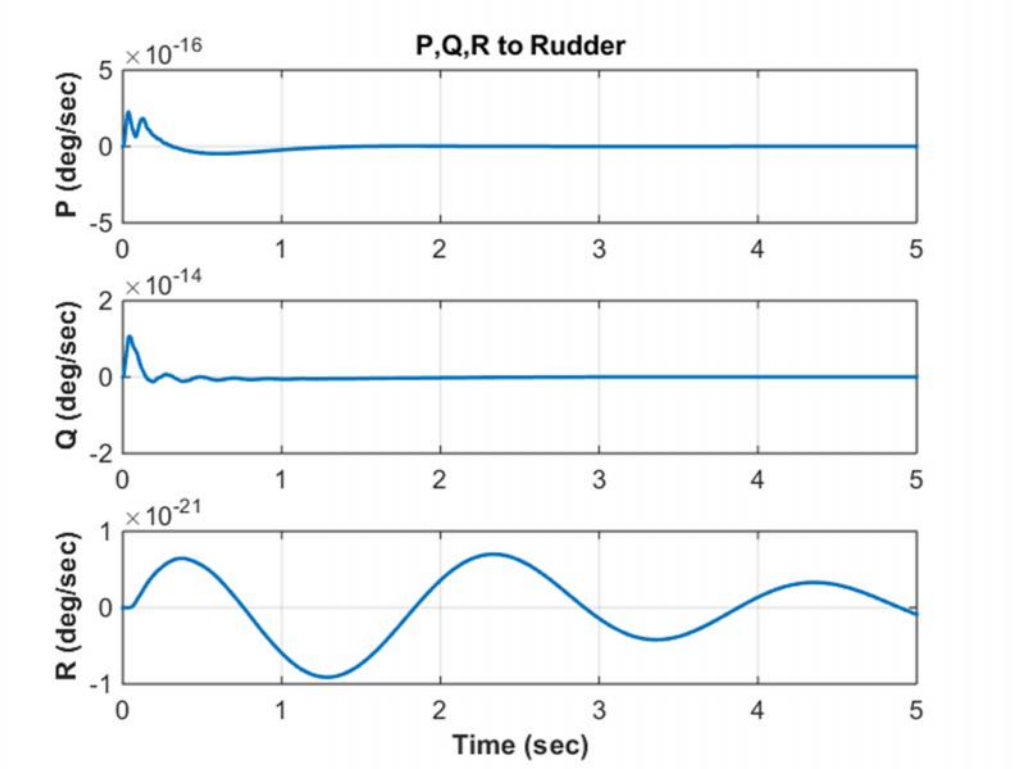

Figure 11: Closed-Loop Step Responses from Rudder (40 kts Case).

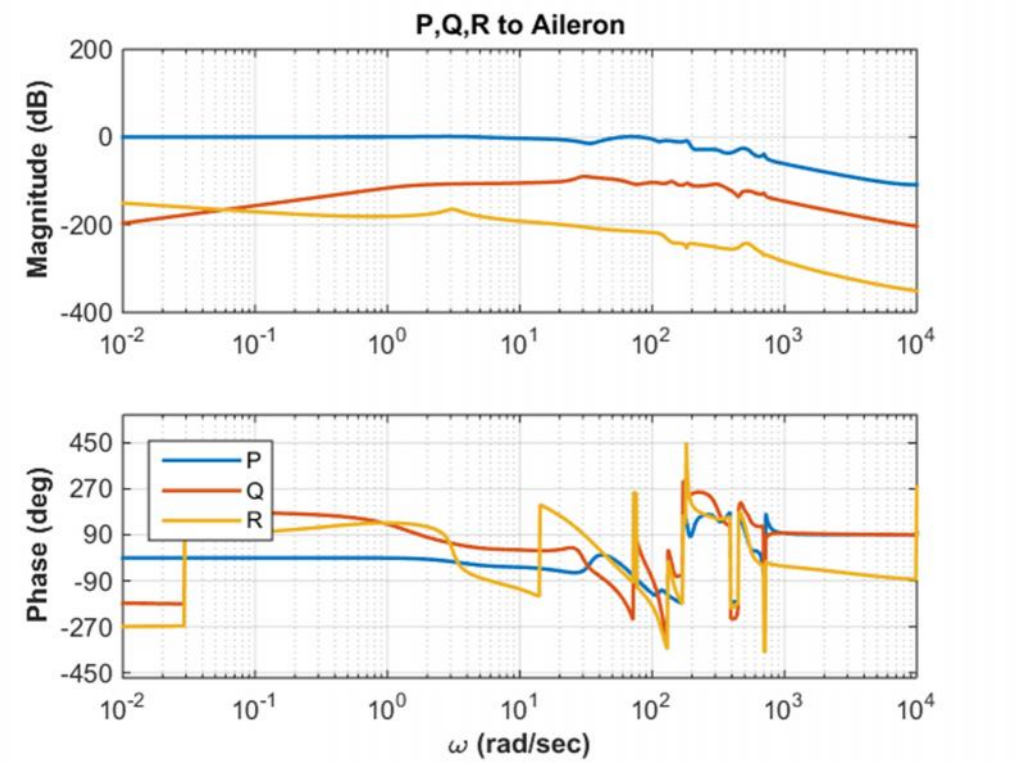

Figure 12: Close-loop Airframe Frequency Responses from Aileron (40 kts Case).

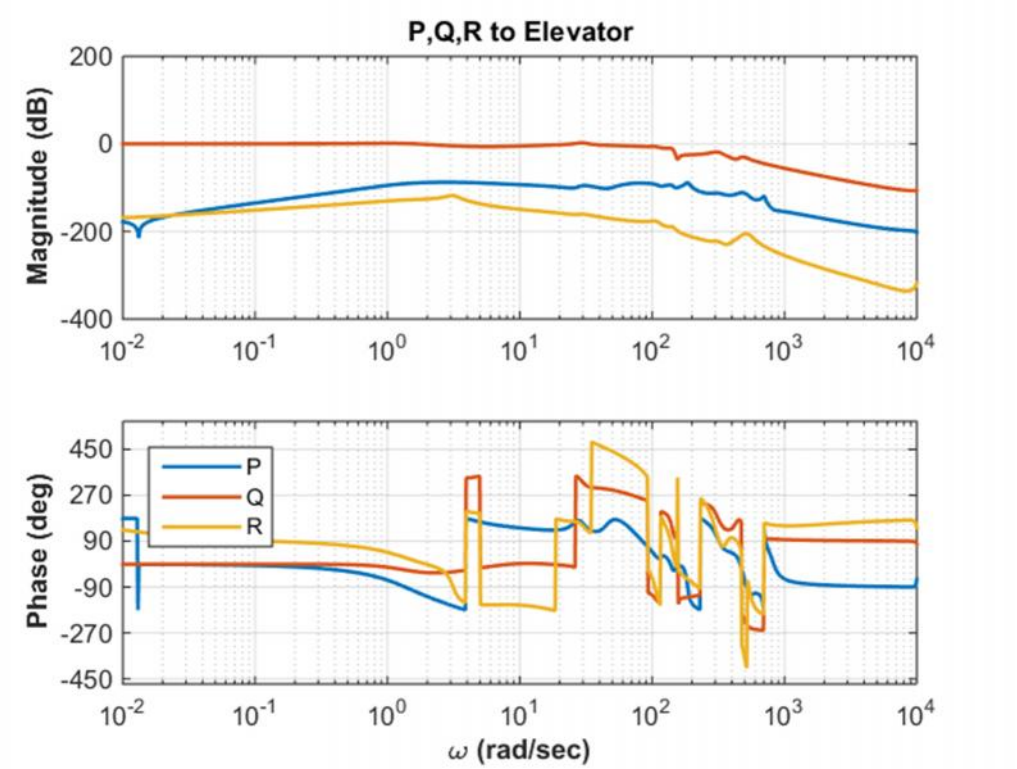

Figure 13: Close-loop Airframe Frequency Responses from Elevator (40 kts Case).

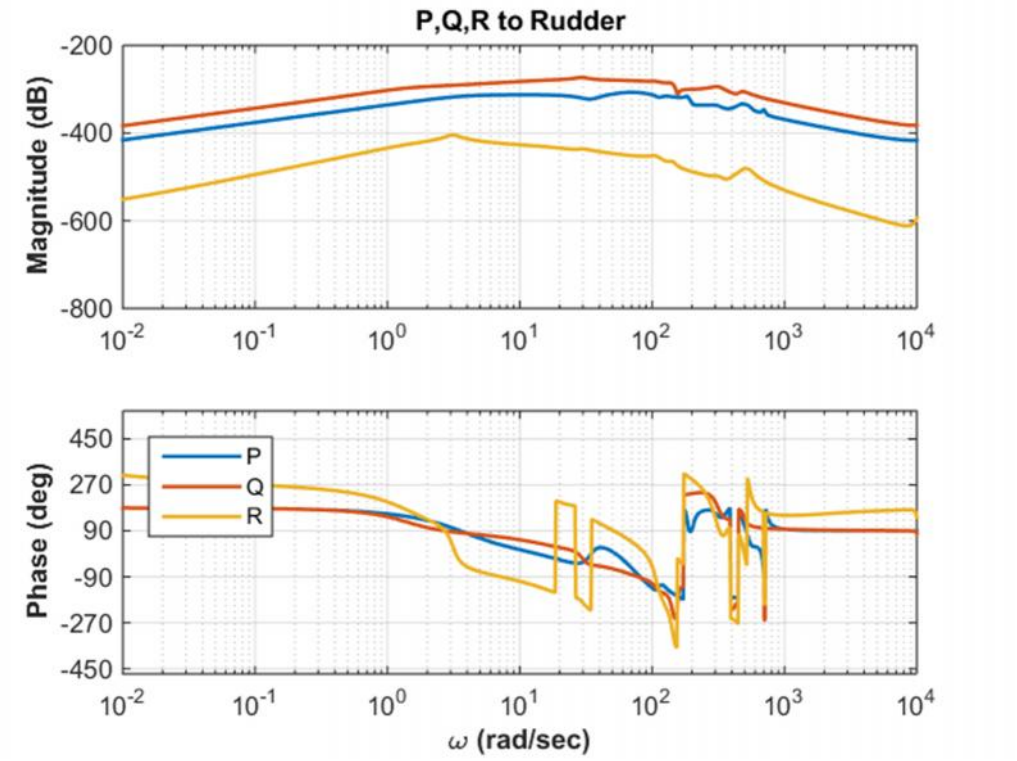

Figure 14: Close-loop Airframe Frequency Responses from Rudder (40 kts Case).

The pole-zero plots of diagonal responses of the close-loop system are presented in Figure 15 to Figure 17. The closed-loop transfer functions for each diagonal input-output pair are shown below in shorthand form

defined as $a(b)[\zeta,\mu]=a(s+b)[s^2+2\zeta\mu s+\mu^2]$. Any minus signs in the transfer function display indicates unstable poles and zeroes. The transfer function shown is after minimal realization to cancel dipoles. There exist unstable poles close to zero at (-0.001224). The other unstable poles ((-0.1083) and (-1.114)) shown in the Q/δe transfer function is due to artifact introduced by minimal realization. It is identified that several non-minimum-phase zeros (shown in bold) exist. To achieve the good controller performance it was necessary to negate the system outputs.

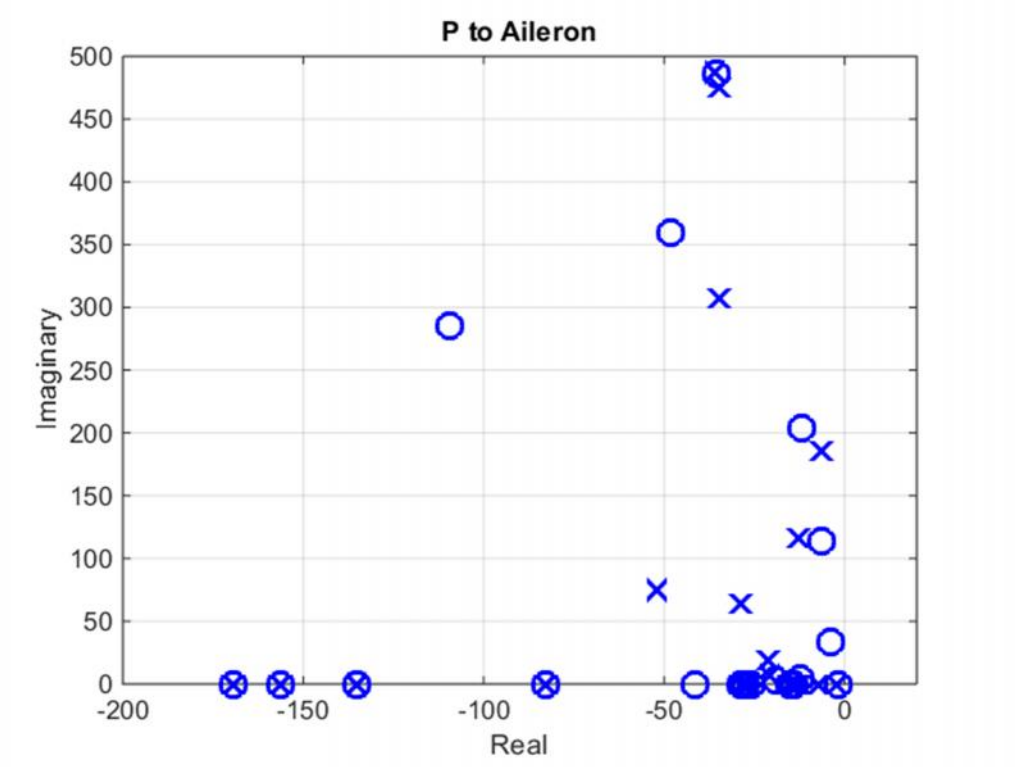

Figure 15: Closed-Loop P from Aileron Pole-Zero Map (40 kts Case).

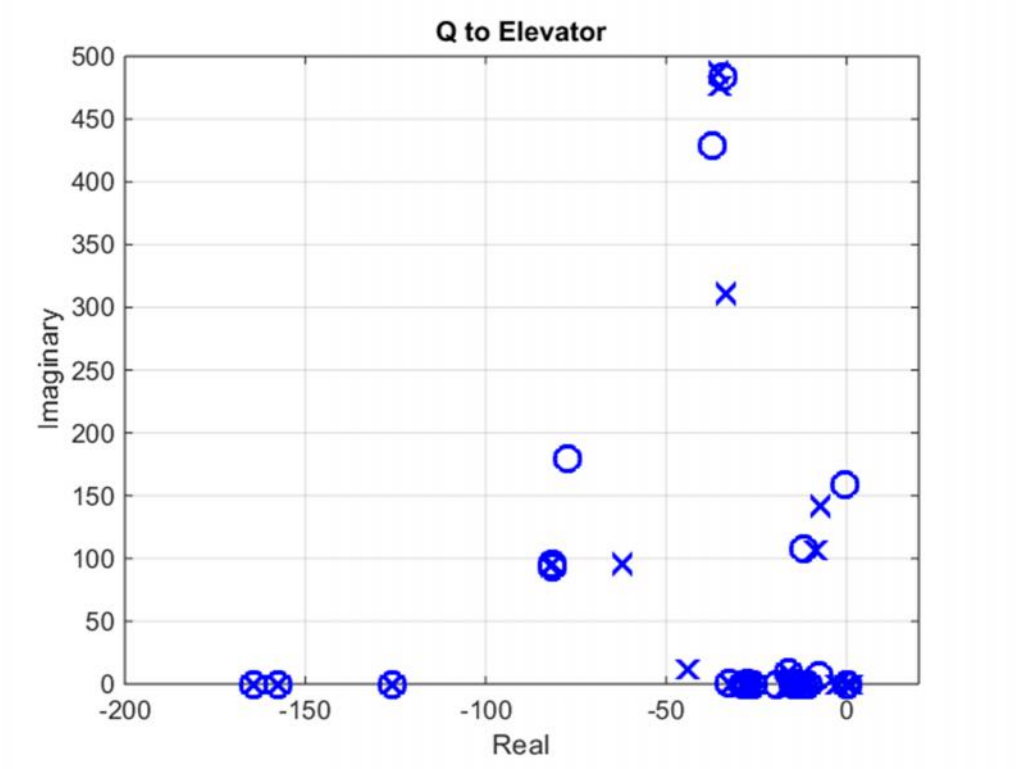

Figure 16: Closed-Loop Q from Elevator Pole-Zero Map (40 kts Case).

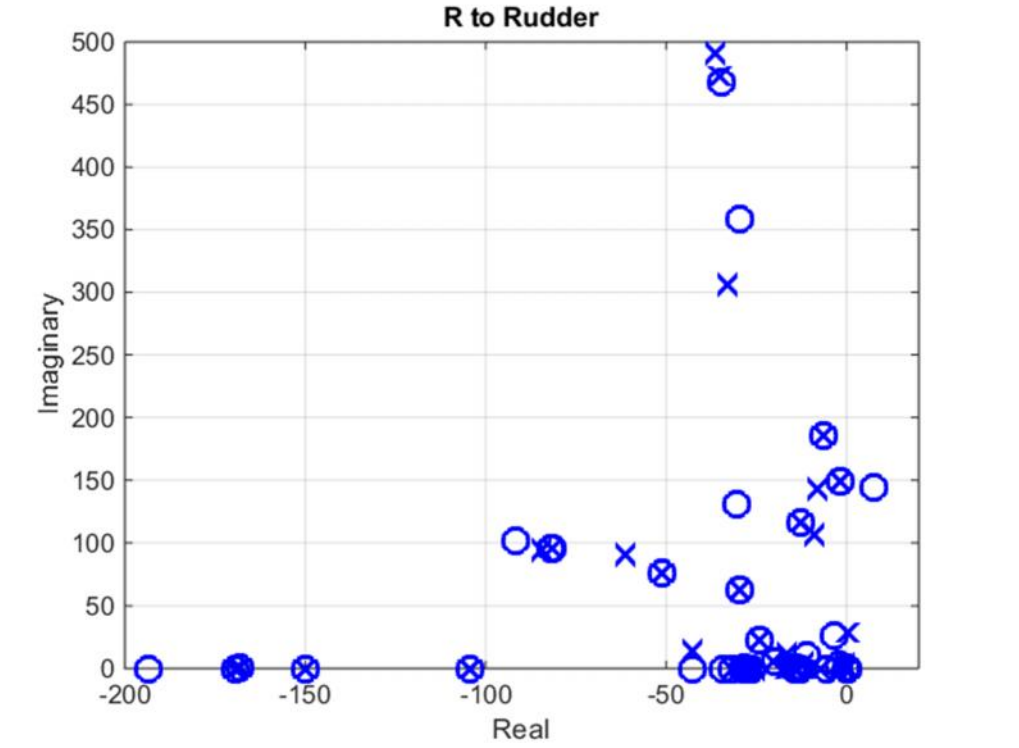

Figure 17: Closed-Loop R from Rudder Pole-Zero Map (40 kts Case).

P/¢a

```
     5.023e+06(1.889)[0.9465,12.82](14.09)(14.12)(14.45)(14.48)(15.07)[0.9865,19.44](26.01)
     (27.32)(27.52)(28.24)(28.24)(28.3)(28.7)[0.1114,33.85](41.65)(82.87)[0.0579,113.5]
     (135.3)(156.5)(169.5)[0.05752,203.8][0.3576,305.6][0.133,363.1][0.07315,487.4]
     (521.1)[0.1194,571.5][-0.06426,706.6](821.2)(984.5)(9802)(-1.016e+04)[0.01019,1.164e+04]
     [0.01007,1.585e+04][0.01001,1.663e+04][0.01041,4.887e+04](-5.488e+04)(5.492e+04)
     [0.01004,7.953e+04][0.01002,9.652e+04][0.01002,9.663e+04]
tf = ----------------------------------------------------------------------------------------
     (2.335)(7.184)(12.6)(14.04)(14.17)(14.44)(14.48)(15.07)[0.9568,21.78](26.03)(27.32)
     (27.59)(28.18)(28.24)(28.28)(28.72)[0.7425,28.76][0.4082,70.14](82.88)
     [0.5718,90.63][0.109,116.7](135.3)(156.5)(169.5)[0.03394,185.2][0.112,309.3]
     [0.07252,476.4][0.07364,488.6](521.1)[0.06711,536.7][0.01715,699.9](821.2)(984.5)
     [0.01017,1.172e+04][0.01002,1.312e+04][0.01006,1.595e+04][0.01,1.668e+04]
     [0.01007,5.18e+04][0.01002,7.996e+04][0.01002,9.647e+04][0.01003,9.663e+04]
     [0.01002,9.664e+04]
```

Q/¢e

```
     5.856e+06(-0.1224)(-0.5162)[0.7754,10.13](10.47)(12.06)[1,14.09](14.47)(14.48)(14.92)
     [0.8811,18.23](19.52)(25.65)[1,27.34](28.24)(28.24)(28.58)[1,32.39][0.109,108.7]
     [0.6574,124.3][0.65,125.7](125.8)(157.7)[0.00397,159](164.4)[0.3955,195.2](296.4)
     [0.08642,430.9][0.07094,484.7](518.6)[0.06747,543](987.7)[0.01056,9743]
     [0.009946,1.471e+04][0.009863,1.611e+04][0.8538,2.374e+04][-0.8377,2.405e+04]
     [0.009805,6.308e+04][0.009918,8.386e+04][0.01002,9.638e+04][0.01002,9.665e+04]
tf = ----------------------------------------------------------------------------------------
     (-0.1083)(-1.114)(2.63)(10.52)(12.18)[1,14.14](14.47)(14.49)[0.9871,15.83](16.08)
     [0.8714,18.28](25.63)(27.32)(27.38)(28.15)(28.24)(28.6)(31.96)[0.9663,45.63]
     [0.08135,106.9][0.5426,114.1][0.6586,124.6][0.65,125.7](125.8)[0.05032,141.7](157.7)
     (164.4)(296.4)[0.107,313.1][0.07349,478][0.07233,488.6](518.6)[0.06793,541.1](987.7)
     [0.01006,1.014e+04][0.01,1.295e+04][0.01005,1.584e+04][0.01,1.707e+04]
     [0.01007,5.178e+04][0.01002,7.973e+04][0.01002,9.637e+04][0.01003,9.663e+04]
     [0.01002,9.665e+04]
```

R/¢r

```
     1.334e-21(1.903e-06)(-0.001238)(0.00126)(0.06195)[0.08113,0.1332][0.7875,3.485]
     [0.4906,3.587][0.9984,13.17](14.07)(14.11)(14.12)(14.27)(14.33)[0.9972,14.41](14.56)
     [0.4082,15.74][0.9629,20.83][0.4722,22.3](26.02)(27.26)(27.48)(27.73)(28.24)(28.26)
     [1,28.26][1,28.46](28.77)(31.53)[0.737,32.98](33.53)(40.84)[-0.02937,57.25][0.4283,68.72]
     [0.5605,91.11][0.7523,100.9](104.4)[0.1568,105.1][0.1079,116.7][0.6506,125.6]
     [0.65,125.7][0.6487,125.9][0.6472,133.6][0.06264,142.8][0.0112,149.1](150.1)[1,168.3]
     (169.4)[0.03405,185.2][0.09725,312.9][0.07503,472][0.02022,515.3](520.8)(520.9)
     [0.06725,536.7][0.07019,552.5](800)(801)(901.6)(965.8)[0.01001,1.018e+04]
     [0.009915,1.299e+04][0.01046,1.545e+04]
tf = ----------------------------------------------------------------------------------------
      (2.496e-06)(-0.001224)(0.001242)[0.2692,0.001826](0.2796)[0.1015,3.12]
      [0.6143,3.706](7.345)[0.9509,12.56][1,14.04](14.11)[1,14.13](14.27)[1,14.47](16.33)
      [0.8323,19.86][0.9635,21](25.54)(27.27)(27.38)(27.48)(28.18)(28.24)[1,28.26](28.27)
      [-0.01534,28.3](28.37)(28.65)(28.77)(31.8)[0.7369,32.98][0.9539,44.68][0.4279,68.78]
      [0.5603,91.07](104.4)[0.08431,106.7][0.562,109.2][0.108,116.7][0.65,125.7]
      [0.65,125.7][0.6499,125.7][0.6645,126.9][0.05556,142.7][0.01121,149.1](150.1)
      [1,168.3](169.4)[0.03407,185.2][0.107,307.9][0.07371,474][0.07384,492.5](520.7)(521)
      [0.06705,536.7][0.06626,552.8](800)(800.9)(901.6)(967.2)[0.01006,1.014e+04]
      [0.01,1.295e+04][0.01005,1.584e+04]
```

2.2 Controller Design for the Model at 44 kts.

The same approach used to design a SAS system at 40 kts was applied to 44 kts case. As the airspeed increases the PI controller fails. As shown in Figure 18 the gain for control allocation is almost identical computed at 40 kts. Figure 19 to Figure 21 are Bode plots from each equivalent control surface to the roll, pitch, and yaw rates. Again, the rudder effectiveness on each angular rate is negligible. From the frequency response plots, the identified two rigid body modes are,

- **stable short-period mode:** $\mu_n = 29.8$ rad/sec, $\zeta = 0.641$
- **stable dutch-roll mode:** $\mu_n = 3.43$ rad/sec, $\zeta = 0.101$

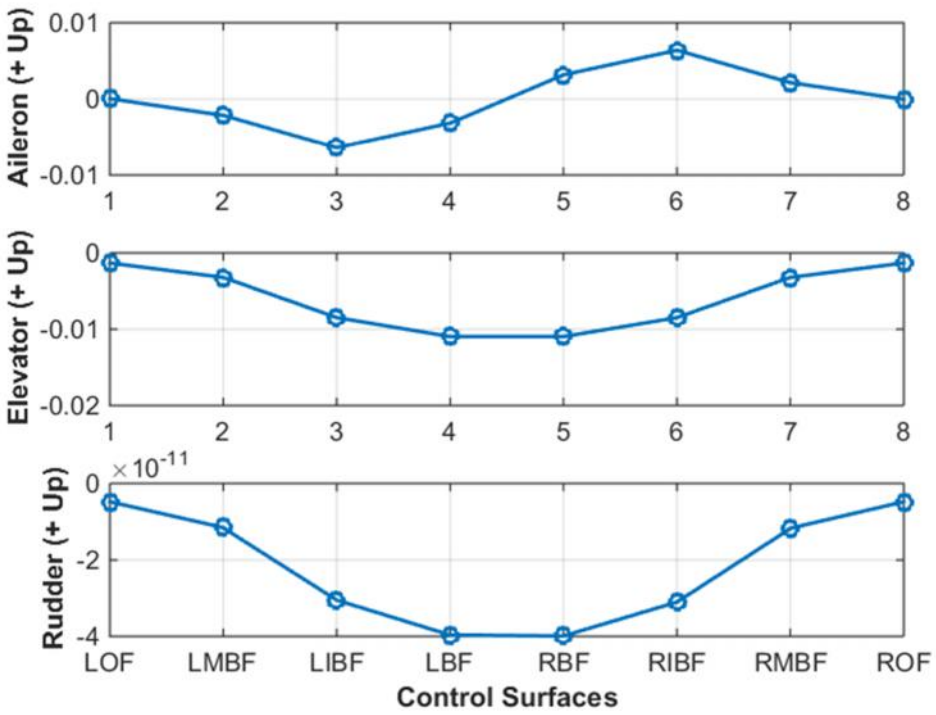

Figure 18: Control Allocation Example (44 kts Case).

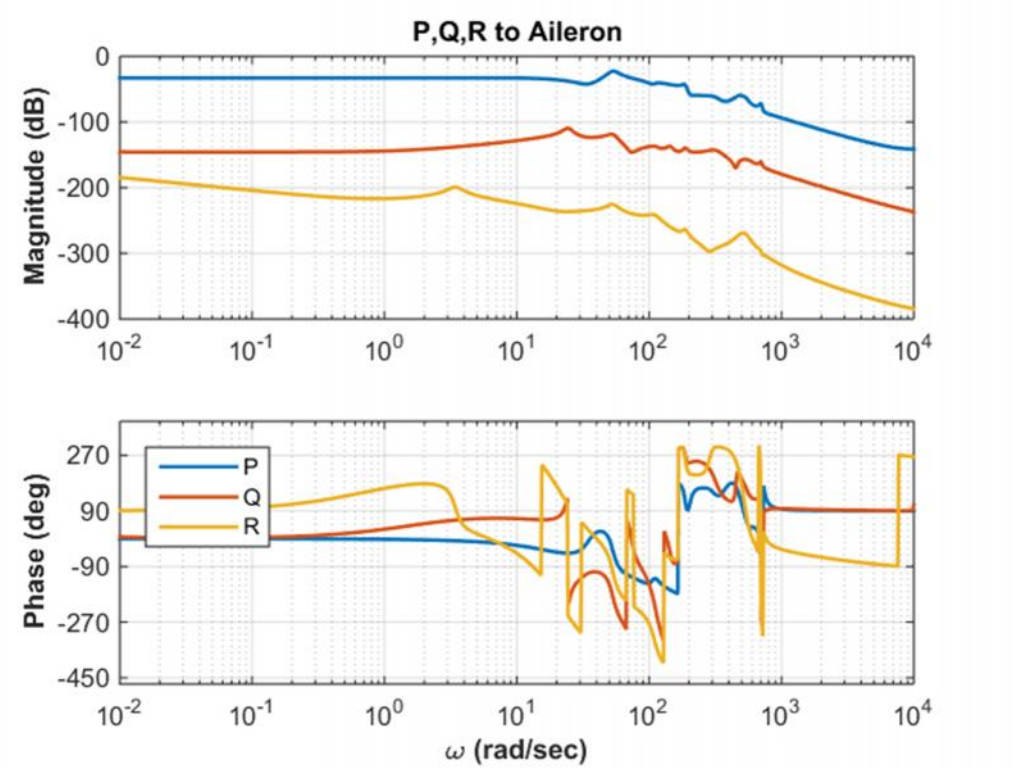

Figure 19: Bare Airframe Frequency Responses from Aileron (44 kts Case).

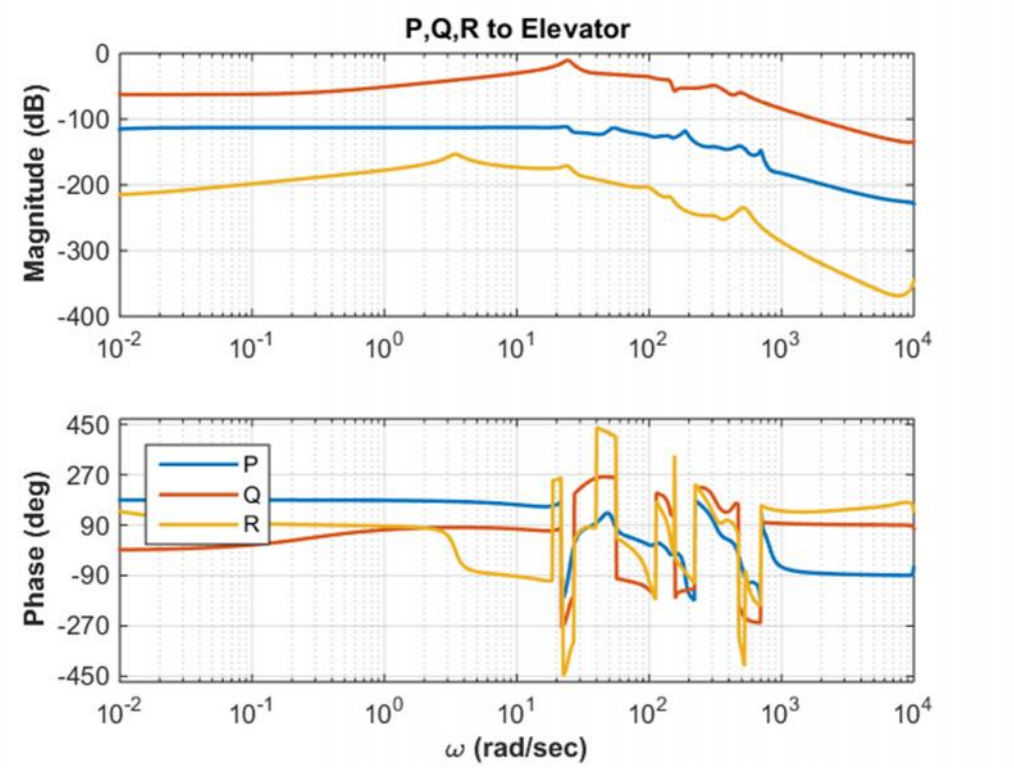

Figure 20: Bare Airframe Frequency Responses from Elevator (44 kts Case).

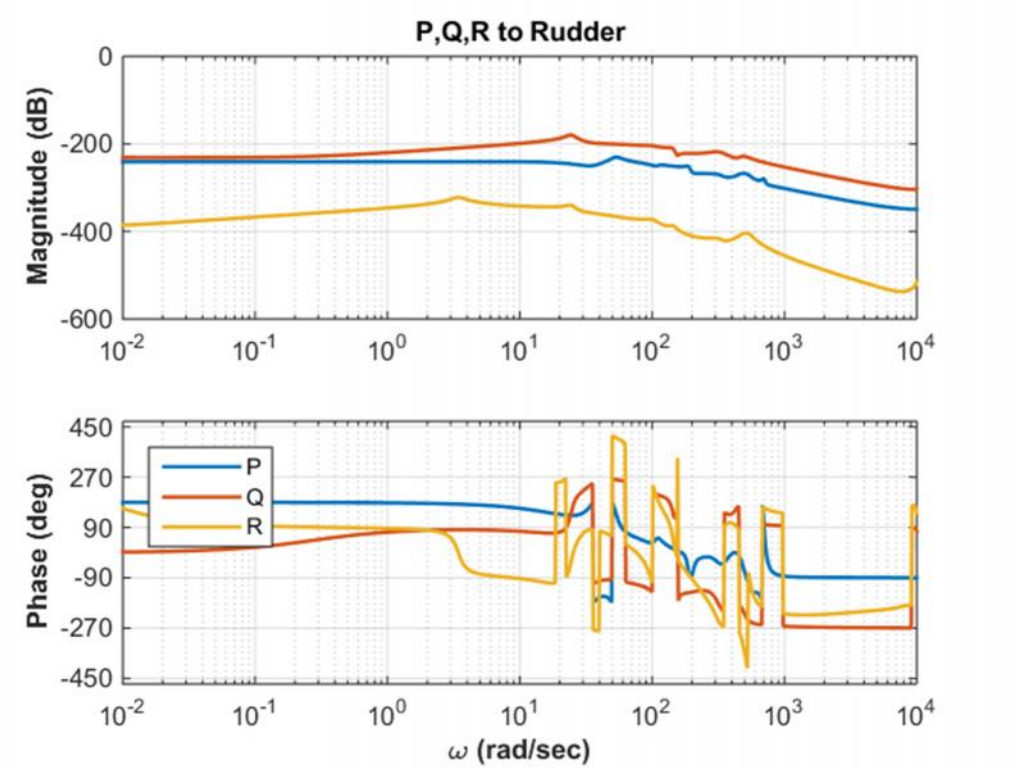

Figure 21: Bare Airframe Frequency Responses from Rudder (44 kts Case).

It should be noted that the fist symmetric bending modes is unstable ($\mu_n = 24.4$ rad/sec, ¸ $= -0.0681$) and coupled with short period mode making the whole system unstable, as shown in the step responses of roll, pitch, and yaw rates presented in Figure 22 to Figure 24. The pitch rate response to equivalent aileron and elevator is unstable. In addition, noted is the cross-coupling effect in roll and yaw axes. The same successive loop-closure technique with the same controller structure is applied to improve command tracking performance as well as to provide stability augmentation on each axis.

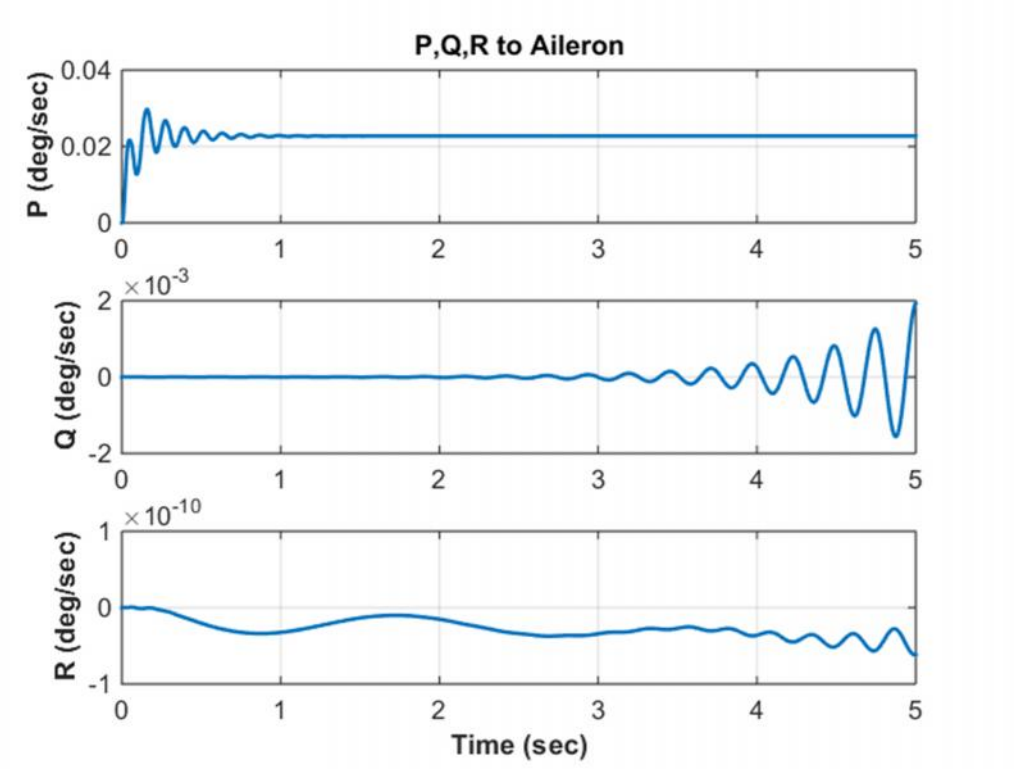

Figure 22: Bare Airframe Step Responses from Aileron (44 kts Case).

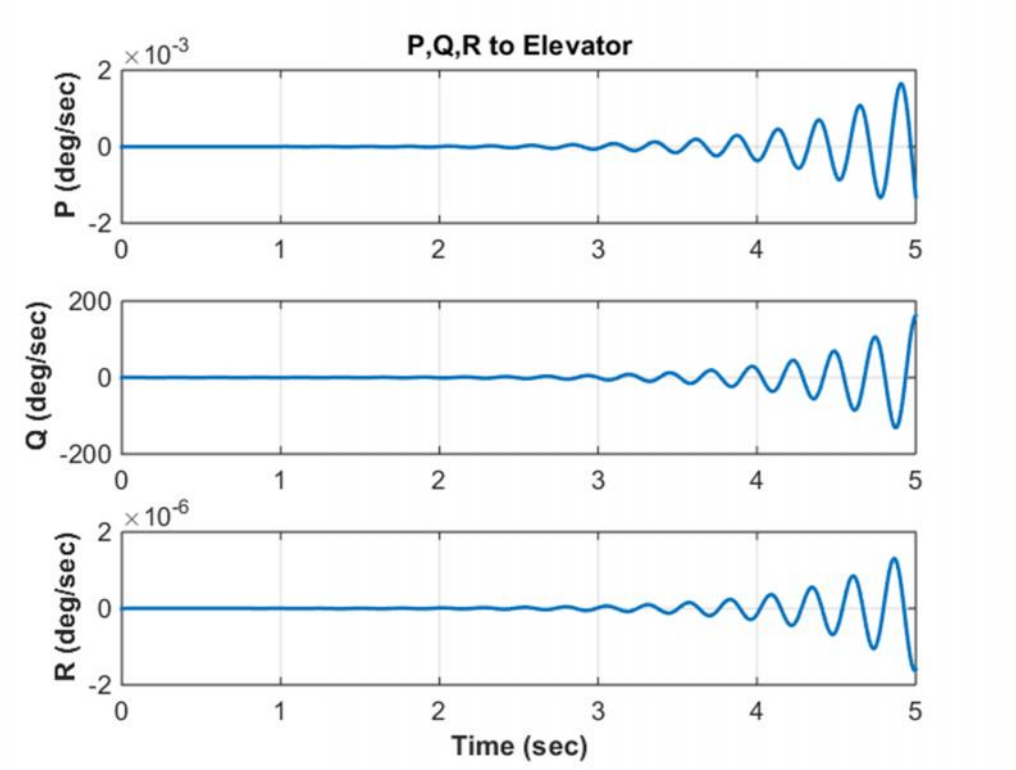

Figure 23: Bare Airframe Step Responses from Elevator (44 kts Case).

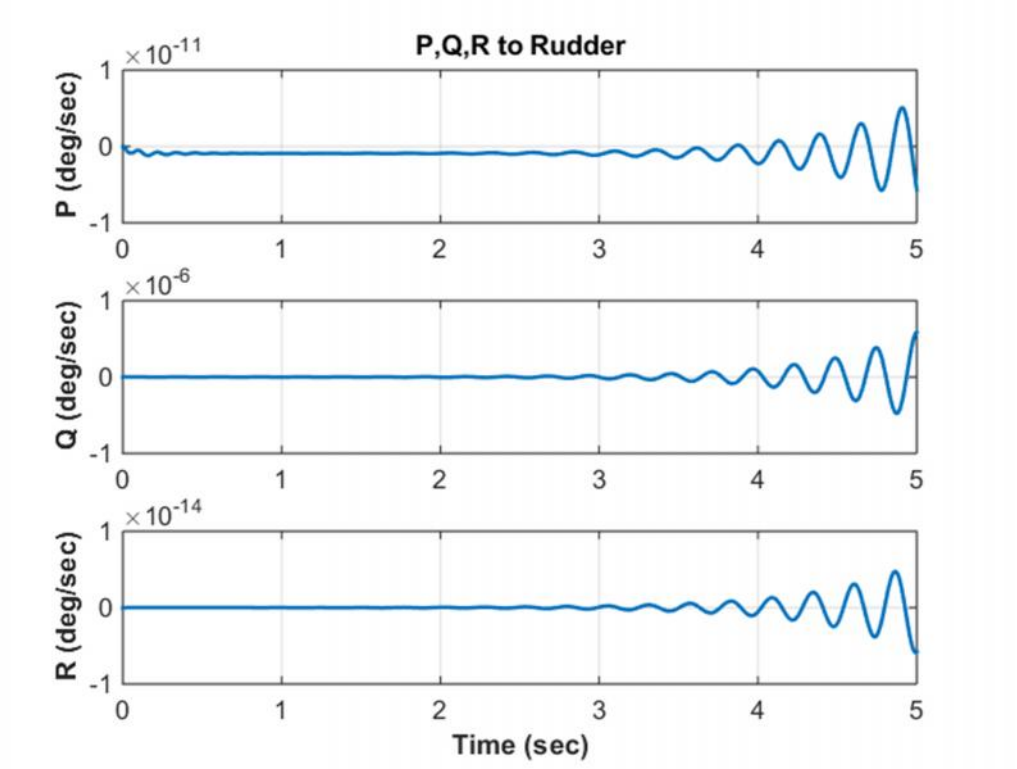

Figure 24: Bare Airframe Step Responses from Rudder (44 kts Case).

Figure 25 to Figure 27 show that the SAS provided a good tracking performance and stability. It is noted that the pitch rate shows oscillatory transient response before it settles to the steady-state condition. Again, Figure 31 to Figure 33 show that the dominant short period mode and the anti-symmetric wing 1st Bending modes at 53.2 rad/sec were successfully suppressed. The pole-zero plots of diagonal responses of the close-loop system are also presented in Figure 28 to Figure 30. The closed-loop transfer functions for each diagonal input-output pair are shown below in shorthand form. There exist unstable poles close to zero at -0.003398 in Q/δe and at -0.001224 in R/δr. Again, nonminimum-phase zeros are indicated in bold.

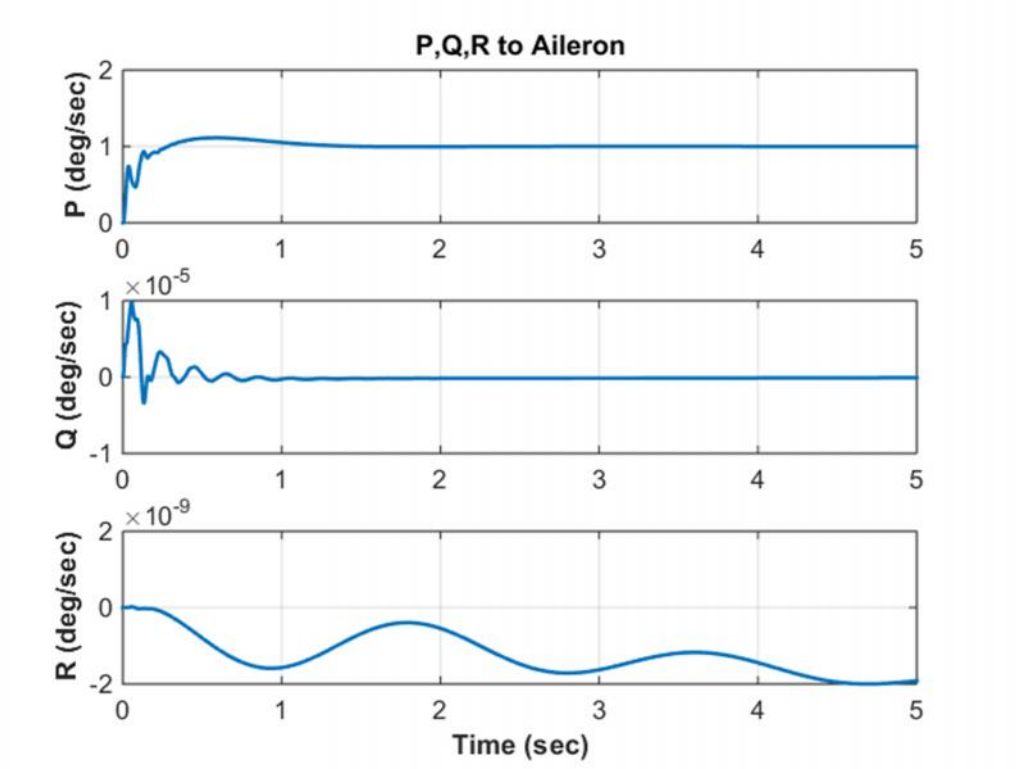

Figure 25: Closed-Loop Step Responses from Aileron (44 kts Case).

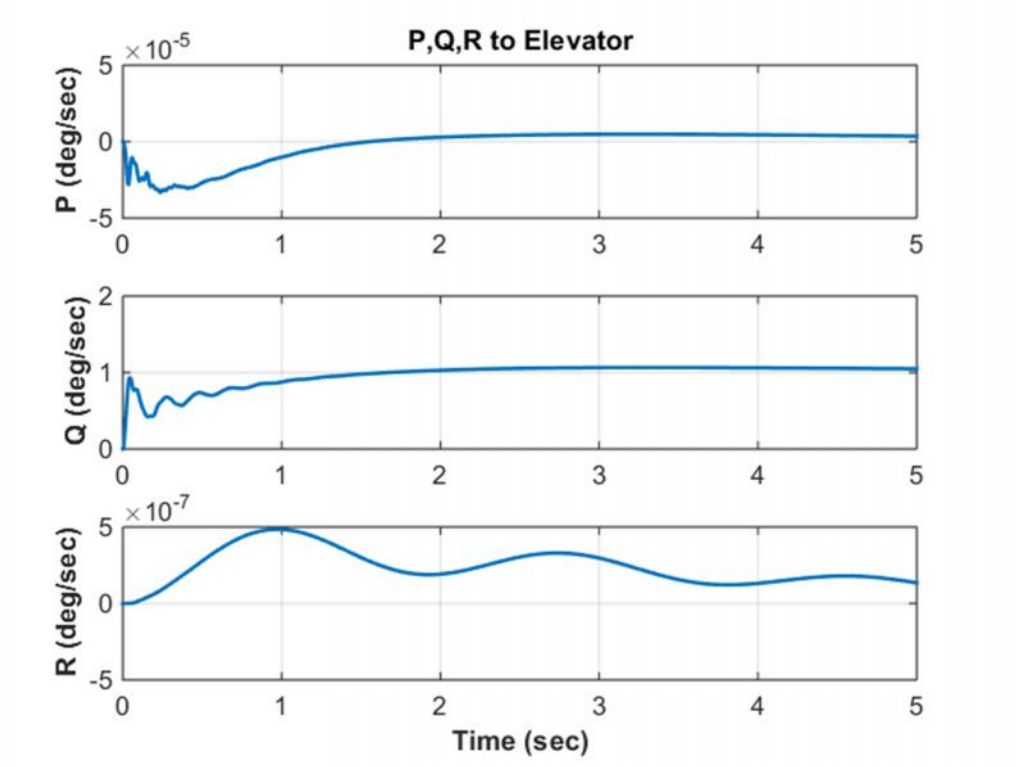

Figure 26: Closed-Loop Step Responses from Elevator (44 kts Case).

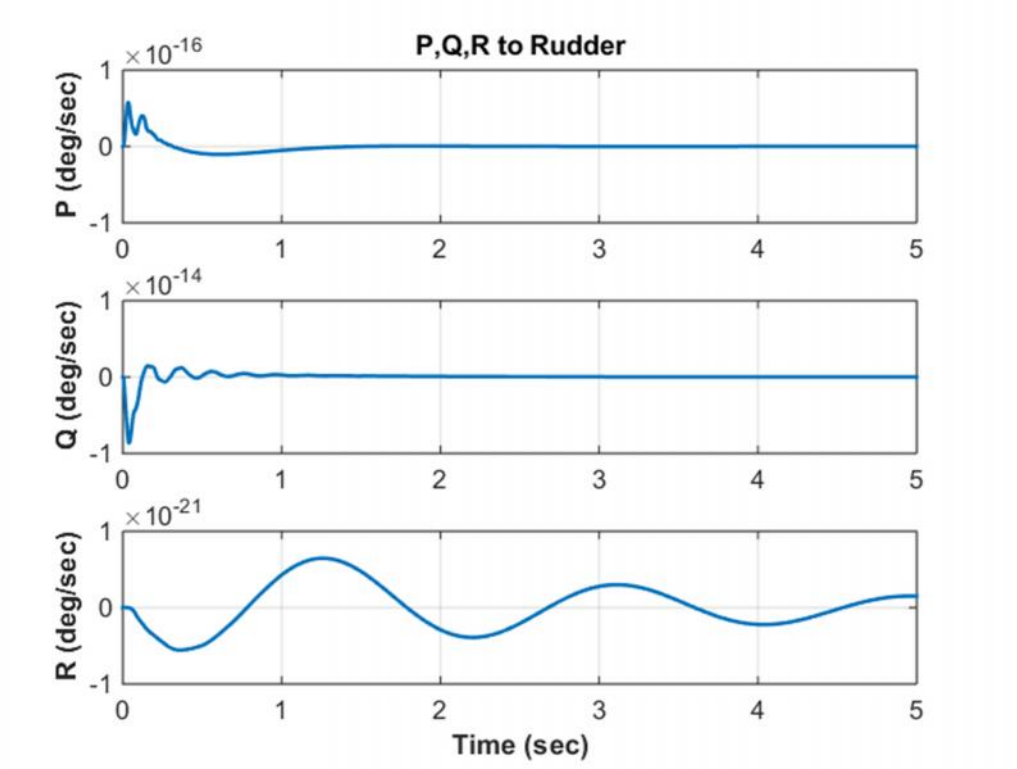

Figure 27: Closed-Loop Step Responses from Rudder (44 kts Case).

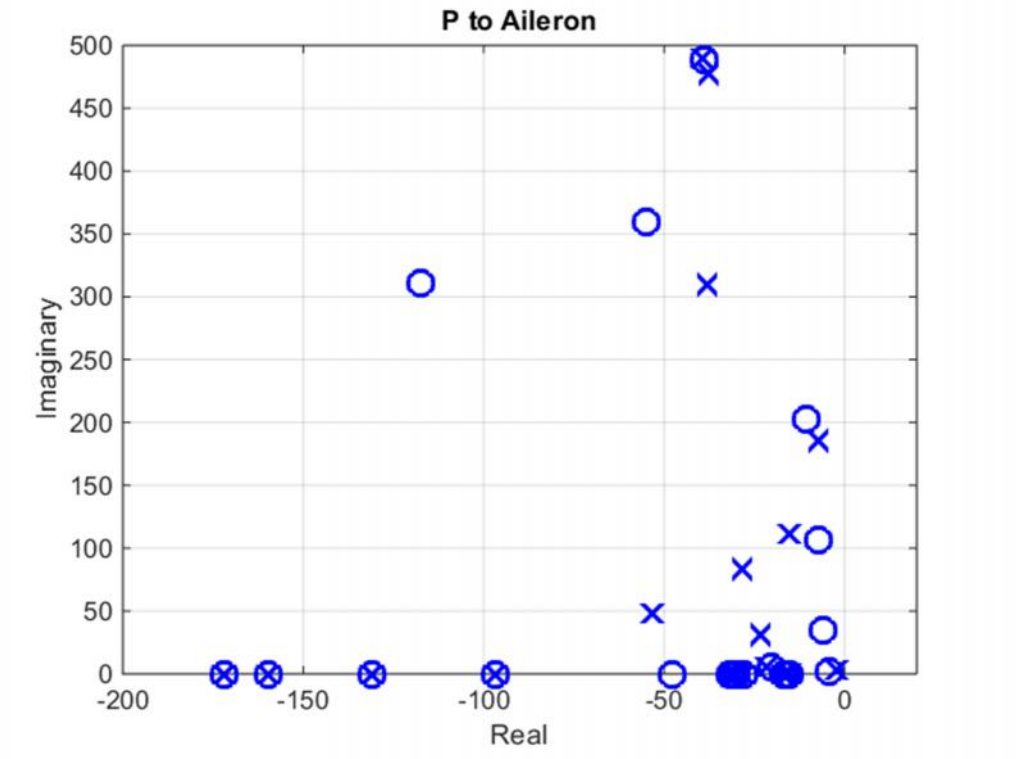

Figure 28: Closed-Loop P from Aileron Pole-Zero Map (44 kts Case).

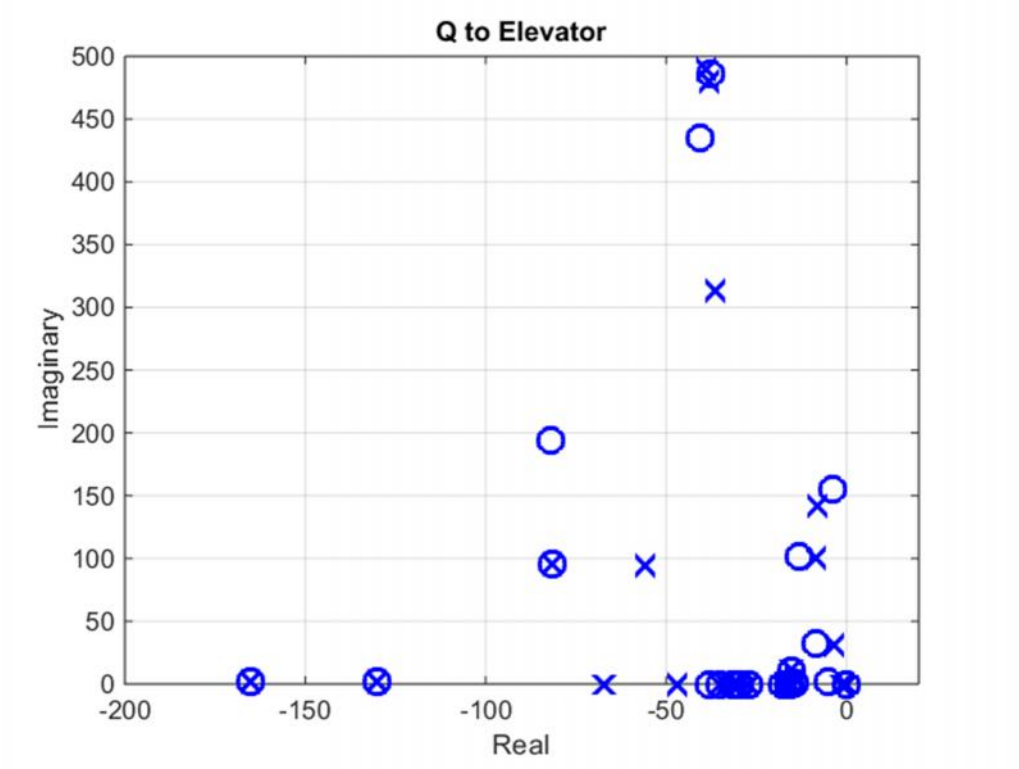

Figure 29: Closed-Loop Q from Elevator Pole-Zero Map (44 kts Case).

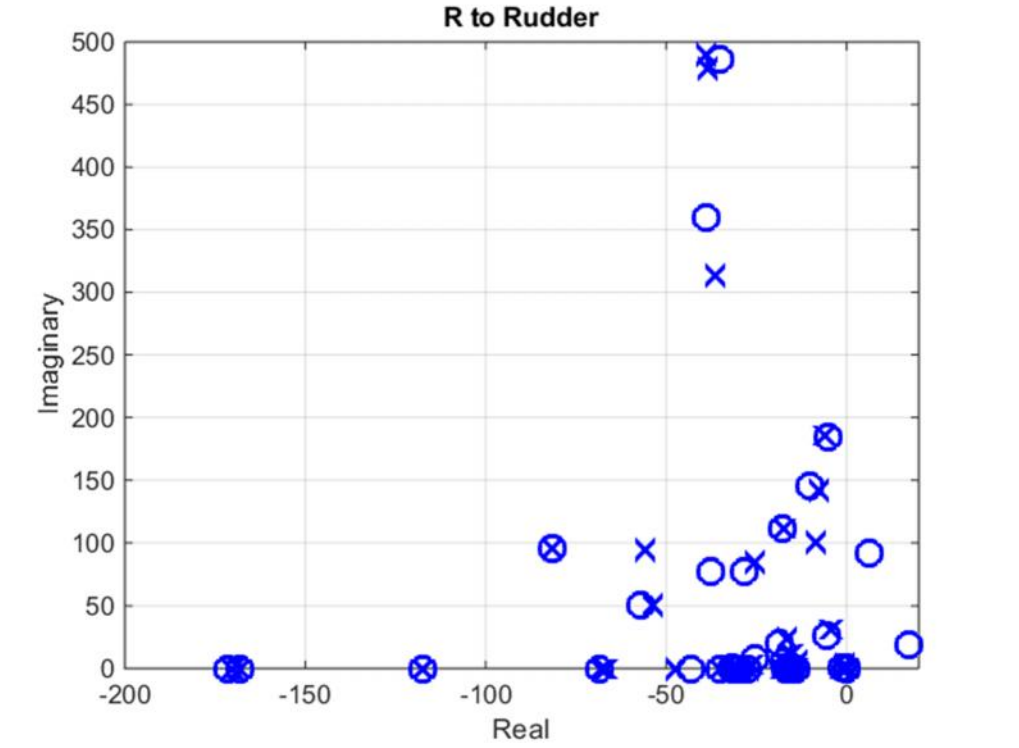

Figure 30: Closed-Loop R from Rudder Pole-Zero Map (44 kts Case).

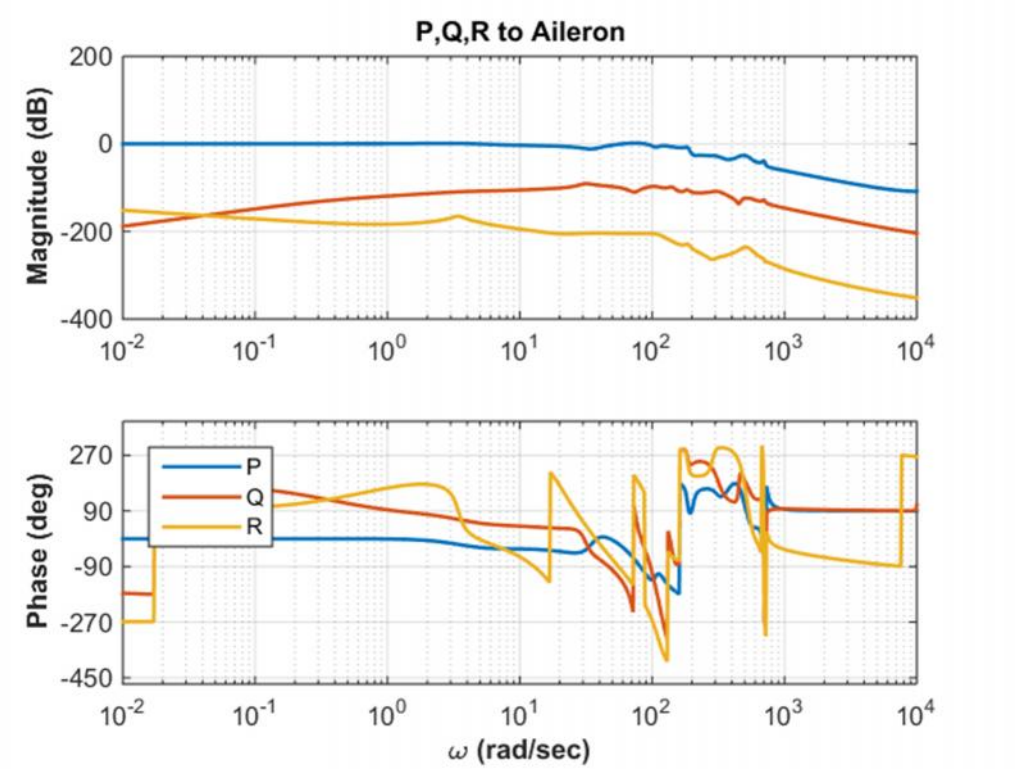

Figure 31: Close-loop Airframe Frequency Responses from Aileron (44 kts Case).

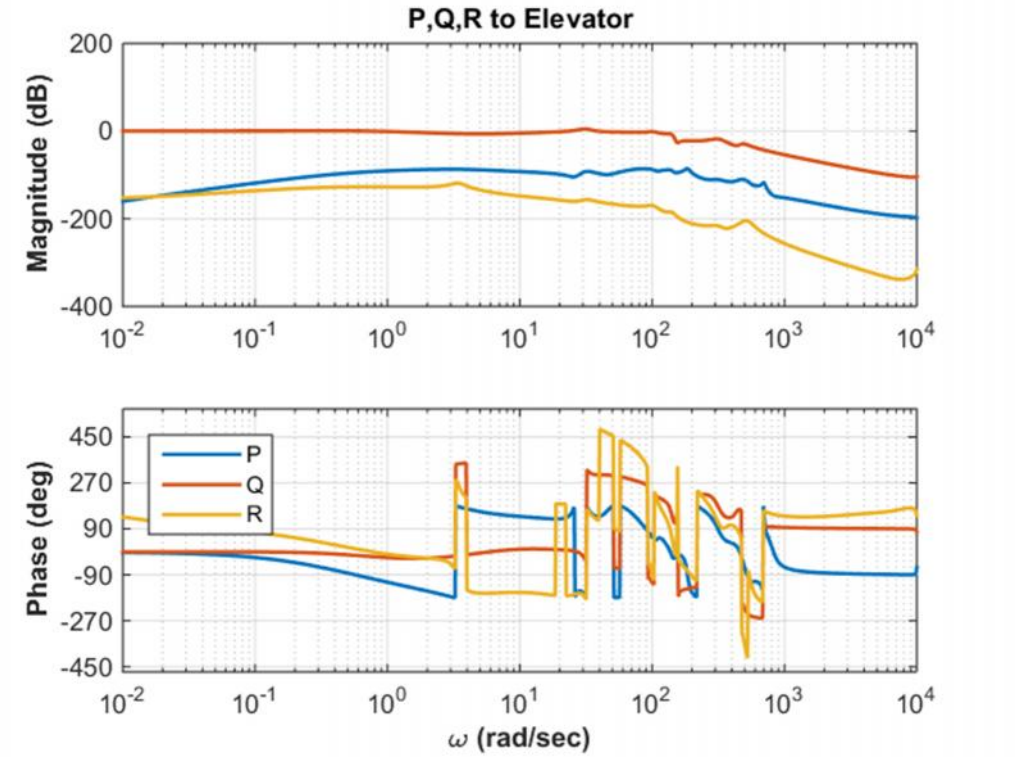

Figure 32: Close-loop Airframe Frequency Responses from Elevator (44 kts Case).

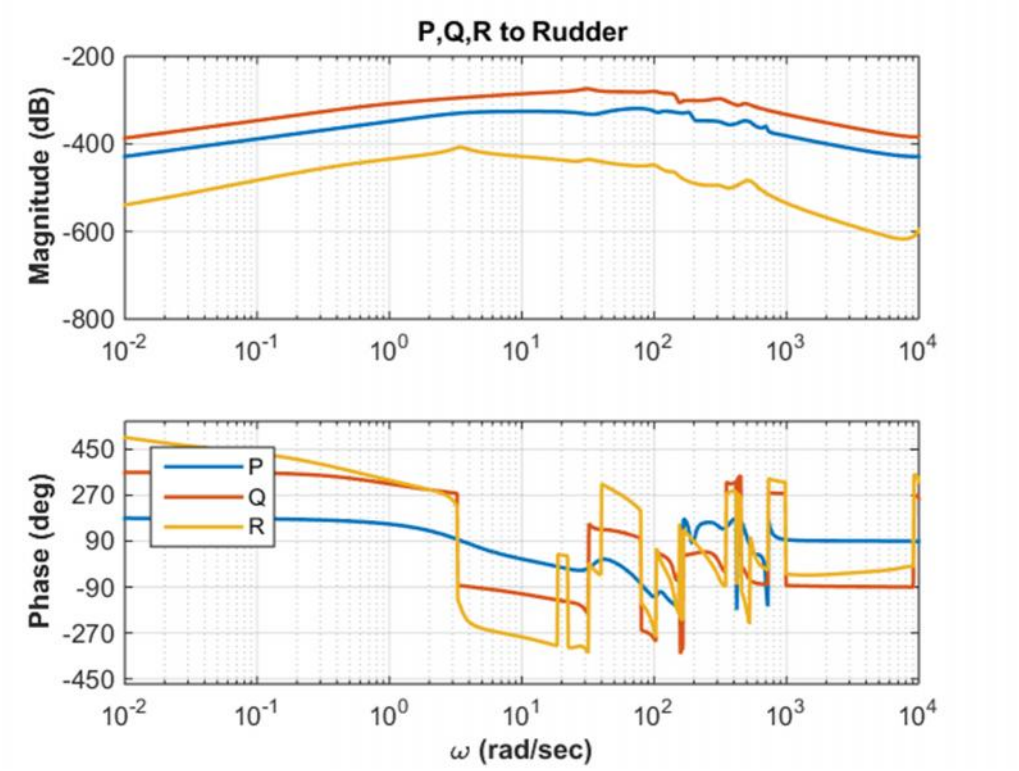

Figure 33: Close-loop Airframe Frequency Responses from Rudder (44 kts Case).

P/¢a

```
      1.953e+05[0.9108,4.702](15.11)(15.41)(15.51)(15.83)(16.02)(16.79)[0.9699,21.17](28.1)
      (29.85)(30.08)(31.07)(31.07)(31.15)(31.72)
      [0.1665,35](47.65)(96.7)[0.0673,106.8](131.2)
      (159.7)(171.8)[0.0518,202.5][0.3539,332.1][0.1505,363.8][0.07967,490.1](519.9)
      [0.1149,567][-0.0534,721.7](800)(941.7)(8885)
      (-9192)[0.01006,1.18e+04][0.0101,1.583e+04][0.01001,1.663e+04][0.009949,5.203e+04]
      [0.01009,7.799e+04][0.01002,9.653e+04][0.01003,9.663e+04](2.893e+05)(-3.043e+05)
tf = ------------------------------------------------------------------------------------
     [0.6595,3.59][1,15.41][0.9999,15.84](16.02)(16.79)[0.9628,22.42](28.13)(29.85)(30.13)
     (31.02)(31.07)(31.12)(31.74)[0.6062,38.45][0.7429,71.68][0.3231,87.78](96.7)
     [0.1361,112.6](131.2)(159.7)(171.8)[0.03825,185.2][0.1221,312.2][0.0789,479.3]
     [0.07998,491.3](519.9)[0.07238,539][0.01797,699.6](800)(941.7)[0.01019,1.172e+04]
     [0.01002,1.312e+04][0.01007,1.595e+04][0.01,1.668e+04][0.01007,5.18e+04]
     [0.01003,7.996e+04][0.01002,9.647e+04][0.01003,9.663e+04][0.01003,9.664e+04]
```

Q/¢e

```
      -4.902e+05(-0.003398)[0.9714,5.343][0.9999,14.22](15.48)(15.51)(16)(16.07)
      (17.66)[0.8325,18.5](27.27)(29.78)(29.92)(31.11)(31.56)[0.2549,32.88](34.99)(38.12)
      [0.1276,101.8][0.65,125.7][0.9998,130.3][0.02575,154.6][0.9999,165.2][0.3902,210.4]
      (436.8)[0.09303,437][0.07716,488][0.07347,544.9](802.7)(1033)
      [0.01007,1.021e+04][0.01016,1.427e+04](1.507e+04)(-1.552e+04)[0.01005,1.588e+04]
      [0.01039,6.28e+04][0.01003,8.07e+04][0.01002,9.638e+04][0.01003,9.664e+04]
      [0.01376,1.483e+05]
tf = ------------------------------------------------------------------------------------
     (-0.003398)(1.393)[0.9593,14.91](14.96)(15.45)(15.59)(16)(16.07)(17.68)[0.811,18.88]
     (27.24)(29.78)(29.92)(31.06)[0.1152,31.36](31.58)(35.05)(47.03)(67.08)[0.08441,101.1]
```

```
     [0.509,109.2][0.65,125.7][0.9998,130.3][0.05558,141.9][0.9999,165.2][0.1157,315.9]
     (436.8)[0.07936,481][0.07949,491.8][0.07372,543.4](802.7)(1033)
     [0.01006,1.014e+04][0.01001,1.295e+04][0.01005,1.584e+04][0.01,1.707e+04]
     [0.01008,5.178e+04][0.01003,7.973e+04][0.01002,9.637e+04][0.01003,9.663e+04]
     [0.01003,9.664e+04]


R/¢r
     2.423e-21(-0.0006003)(0.0008991)[-0.04543,0.001069][0.4802,0.5283](0.7938)
     (1.536)(13.75)(13.87)[0.9409,14.57](14.65)(15.44)(15.53)(15.55)(15.58)(15.99)(16.09)
     (17.81)[0.8081,18.71][0.9931,26.63](27.24)[0.5611,29.37](29.78)(29.94)(31.02)(31.06)
     (31.11)(31.57)[0.129,31.76](33.16)(35.06)(47.15)(66.86)(68.22)[0.7304,73.5]
     [0.2912,87.74][0.08506,101.2][0.5083,110][0.1546,112.8](117.5)[0.6502,125.6]
     [0.6499,125.7][0.6497,125.7][0.6501,125.7][0.05534,142](168.2)(170.3)[0.03168,185]
     (206.5)[0.1157,315.1][0.07982,479.7][0.0792,491.2](521.9)(522.6)[0.07379,543.9]
     (800.6)(800.9)(941.2)(964)[0.01006,1.014e+04][0.01001,1.295e+04][0.01005,1.584e+04]
tf = ------------------------------------------------------------------------------------
     [0.485,0.0005238](-0.001224)(0.001242)[0.4909,0.5307](1.533)[0.1015,3.432]
     [0.9987,13.81][0.9399,14.56](15.44)[1,15.54](15.55)(15.58)(16)(16.1)(17.92)[0.8069,18.68]
     [0.994,26.57](27.15)[0.5615,29.35](29.78)(29.92)(31.02)(31.07)(31.1)(31.21)(31.57)
     [0.1288,31.76](35.06)(47.14)(66.9)(68.21)[0.7304,73.51][0.2913,87.75][0.08491,101.2]
     [0.5083,110][0.1545,112.8](117.5)[0.6502,125.7][0.6499,125.7][0.6502,125.7]
     [0.6497,125.7][0.0554,142](168.2)(170.3)[0.03166,185](206.4)[0.1157,315.1]
     [0.07981,479.7][0.07924,491.2](521.9)(522.5)[0.0737,544](800.6)(800.9)(941.1)(964)
     [0.01006,1.014e+04][0.01001,1.295e+04]
     [0.01005,1.584e+04]
```

3.0 CONCLUSION AND FURTHER RECOMMENDATION

The difficulty of designing a SAS for the BFF rigid body modes comes from non-minimum phase zeros and cross coupling between the rigid body modes and the structural modes. The initial feasibility test with a PI controller shows that the PI controller was able to provide good tracking performance and stability below 46 kts. As the airspeed increases the PI controller fails due to excessive coupling between the structural modes and the rigid body modes, as well as unstable structural modes. An effective strategy would be to first suppress the lightly damped (or unstable) aeroelastic modes in an inner loop and then design a SAS in an outer loop.

REFERENCES

[1] Dongchan Lee, and Brian P. Danowsky, STI-Working Paper 1407-14: Open Loop Analysis Survey of GVT-updated X-56A State Space Models for Primary Piloted Operation, May 14, 2013.

[2] Kuo, Benjamin C. *Automatic control systems*. Prentice Hall PTR, 1981.